Fan Broadband Noise Prediction for the ACAT1 Fan Using a Three-Dimensional Random Particle Mesh Method

Carolin A. Kissner*and Sébastien Guérin†
German Aerospace Center (DLR), Berlin, Germany

Fan broadband noise, in particular rotor-stator-interaction noise, is an important broadband noise source in modern aircraft engines. It is, however, still challenging to correctly predict. Analytical tools rely on assumptions, while fully scale-resolving methods are demanding in computing resources. A RANS-informed synthetic turbulence method strives to find a compromise between accuracy and cost. In the past, the authors have used a two-dimensional (2D) approach based on the fast Random Particle Mesh (fRPM) method. While the 2D approach can be performed on a regular personal computer and has yielded good agreement with experimental results, some difficulties remain: Firstly, the quality of the prediction highly depends on the chosen radial position at which a simulation is performed, and the determination of a truly representative radial position is not trivial. Secondly, the 2D approach neglects three-dimensional (3D) flow effects and the turbulence is confined to 2D space. To tackle these issues, the authors expanded the method to three-dimensional space. An effort was made to optimize the used settings in order to achieve accurate results while keeping the computation cost within reasonable limits. These findings were then verified by comparing the synthesized turbulence to analytical data for typical flow and turbulence characteristics found in the interstage region of a fan. The 3D synthetic turbulence method was subsequently applied to a realistic fan configuration. The results of the fan broadband noise prediction were compared to the results of an equivalent 2D simulation. Lastly, the sound power level spectra of the numerical simulations were compared to a sound power level spectrum computed from experimental data.

I. Introduction

Modern Ultra-High Bypass-Ratio (UHBR) engines have larger-than-ever bypass ratios to achieve maximum efficiency. While this trend towards larger engine diameters reduces some sound sources, it can have an adverse effect on fan noise.

The tonal components of fan noise occur at discrete frequencies. The tones have thus been extensively studied by numerical means or in experiments. This led to the development of successful noise abatement techniques. When tones are reduced, the relative contribution of fan broadband noise increases. Compared to fan tones, the understanding of the fan broadband noise mechanism is less advanced. This can be partly attributed to the fact that broadband noise produced by turbulent vortices and therefore more challenging to predict. Applied methods range from analytical to fully-scale resolving techniques. Analytical methods are fast but are restricted to simplified flows and geometries. Fully-scale resolving methods have the potential of completely capturing the physics of the problem but are still expensive.

Synthetic turbulence methods can be seen as a compromise between cost and accuracy. They are typically hybrid approaches, which address each aspect of a physical problem with a separate, highly specialized method. In general, synthetic turbulence methods that are used for studying broadband noise resulting from the interaction of turbulence with the leading edges of blades work as follows: Turbulence is typically

*Research Engineer, Institute of Propulsion Technology, Department of Engine Acoustics, Müller-Breslau-Str. 8, 10623 Berlin, Germany, carolin.kissner@dlr.de.
†Senior Research Scientist, Institute of Propulsion Technology, Department of Engine Acoustics, Müller-Breslau-Str. 8, 10623 Berlin, Germany.

synthesized upstream of the stator leading edges by means of filtering,[1,2] superposition of random Fourier modes (stochastic noise generation and radiation[3–5]), or synthetic eddies.[6–8] The turbulence is then convected in the flow by a Computational AeroAcoustics (CAA) code until the turbulence interacts with the stator geometry. The far field sound can either be analyzed by propagating the sound waves from the source to sensors in the far field or by using a Ffwocs-Williams-Hawkings (FWH) technique using the pressure fluctuations on the stator surface.

In recent years, strides were made to improve these techniques to achieve better broadband noise predictions and to further the understanding of the noise generation mechanism. Only a thorough understanding of fan broadband noise will lead to the development of effective noise abatement techniques. One particular focus has been the expansion of the synthetic turbulence methods to 3D space, which allows for the realization of more realistic turbulence. While the literature shows that these 3D simulations were, in fact, successful, it also highlights one common difficulty: The computations tend to be quite costly, in particular when compared to 2D computations.

I still need to add some relevant literature here regarding expansion of methods to three-dimensional space, key findings of these studies, comparison with 2D simulations, and computation costs. Check for new publication (AIAA 2018).

Last year, Kissner et al.[9] presented an enhancement of the two-dimensional fRPM-fan method, which is a synthetic turbulence method based on the Random Particle Mesh Method[10] and is highly specialized for the prediction of fan broadband noise. For the first time, 2D simulations were performed at several radial position to get a more complete description of the emitted sound in the entire bypass duct. In addition, a correction technique was introduced, which was applied for considering 3D flow effects. In essence, the enhanced technique's aim was to correctly approximate the sound of a 3D problem with a 2D approach. However, even an enhanced and corrected 2D simulation cannot consider effects due to complex 3D geometrical features like serrations. A 3D approach is needed for such cases.

In this paper, the authors build on this previous work by expanding the fRPM-fan method to 3D space. The following questions will be addressed:

- How can the setup of a 3D fRPM-fan simulation be optimized in terms of accuracy and computation cost?
- Do these optimized settings perform as intended?
- How do the results of the fan broadband noise prediction differ when using a 3D as opposed to a 2D approach?
- How well do the numerical results agree with measurement data?

In order to optimize the setup of a 3D simulation, extensive numerical and analytical parameter studies are performed to identify the most relevant factors that influence accuracy and computation cost. The findings are then used to design an optimization routine, which delivers computationally optimal settings for a set of given accuracy specifications. To validate that a simulation using these optimized settings performs as intended, a synthetic turbulence benchmark case is designed. Turbulence statistics and mean flow variables are provided for the interstage section of a real fan. The provided input are needed to validate that the synthesized turbulence agrees with the specifications.

In a next step, the 3D fRPM-fan method is applied to predict the rotor-stator-interaction broadband noise of a real fan configuration, namely the AneCom AeroTest Rotor 1 (ACAT1). The results are compared to the results of an equivalent 2D simulation and to results determined from measurement data.

II. Overview of fRPM-fan method

The fRPM-fan method refers to the fRPM-based synthetic turbulence method that is specifically suited for fan applications. Note that the overview given here is therefore not representative for all fRPM-based techniques. The method is essentially a hybrid method consisting of three separate methods: the Computational Fluid Dynamics (CFD) method, the fast Random Particle Mesh (fRPM) method, and the Computational AeroAcoustics (CAA) method.

A RANS or URANS simulation simulation computes the mean flow and turbulence statistics required as inputs for the fRPM and CAA methods. The fRPM method is a fast implementation of the Random

Particle Mesh (RPM) method, which uses recursive filters on a Cartesian grid to speed up simulations.[11] The fRPM method for fan applications does not directly model source terms but synthesizes time-space-dependent turbulence upstream of the stator row. It works as follows: White noise is scaled by a local variance, i.e. a turbulent kinetic energy, and then spatially filtered by a local length scale. Several Gaussian filters of different filter lengths can be superposed in order to realize a target spectrum, typically a von Kármán spectrum.[12] The variance of each filter depends an analytical weighting function.

The convection of the synthesized turbulence, the sound generation, and the sound propagation was computed using the CAA solver PIANO.[13] In this work, the linearized Euler equations (LEE) are solved. A fourth order low-dispersion low-dissipation Runge-Kutta scheme[14] was used for the time integration and the dispersion-relation-preserving finite difference scheme by Tam and Webb,[15] for the spatial discretization. The fluctuating velocity fields are solenoidally coupled into the CAA domain by adding a relaxation term to the impulse equations as proposed by Ewert et al.[16]

The sound is generated when the turbulence interacts with the leading edge of a stator vane. The sound is then propagated to sensor positions in the far field region to determine sound power levels. Note that the method is technically not restricted to the consideration of rotor-stator-interaction noise, which results from the interaction of the wake turbulence with the stator leading edges. In fact, broadband noise resulting the interaction of ingested turbulence (ingestion noise) or boundary layer turbulence with the leading edges of the stator can also be considered.

The fRPM-fan method is also capable of considering cyclostationary mean flows and turbulence statistics as demonstrated in several papers.[9,17,18] This extension of the method will, however, not be employed in this work.

III. Validation of 3D turbulence synthesis

In this section, the goal is to verify that 3D turbulence is synthesized accurately with minimal computation effort. In the framework of the EU project TurboNoiseBB, a so-called synthetic turbulence benchmark case was designed. The test case was intended to be used to test synthetic turbulence methods by validations with analytical turbulence. Before performing the benchmark case, various numerical and analytical parameter studies were performed to optimize the simulation settings in terms of accuracy and computation cost. The key findings will be presented and applied for the fan noise simulation.

A. Specifications of synthetic turbulence benchmark case

In close collaboration with other partners, DLR set up a synthetic turbulence benchmark case. The goal was to provide a common turbulence that is realistic for an interstage region and can be used to test the synthesized turbulence. It was specifically intended to test methodological advancements.

A RANS simulation of the ACAT1 fan was performed at modified approach conditions featuring a slightly increased bypass flow in order to avoid any flow detachments near the rotor tip. The simulation was performed using the DLR in-house CFD solver TRACE.[19] A mixing-plane approach was used and the Menter SST k-ω turbulence model[20] was applied. The ACAT1 fan has 20 rotor blades, 44 stator vanes, and 44 engine support stator (ESS) vanes. Turbulence statistics (turbulent kinetic energy and turbulent length scale) and primitive mean flow values (density, velocities, and pressure) were extracted at the position marked in green in Figure 1. Since the synthetic turbulence method is to be applied to only the bypass flow, the core flow was discarded. To separate the core flow from the bypass flow, a streamline was computed at the stator hub wall (shown in red in Figure 1). As a perfectly annular duct will be considered for the synthetic turbulence benchmark case, radial velocities are set to zero to avoid conflicting states at the walls of the CAA domain. To ensure that the flow fulfills the Euler equations, the pressure was corrected using a technique that has e.g. been presented by Tam and Auriault.[21] Axial and circumferential velocities remained unchanged. With the exception of the turbulent length scale, all variables were circumferentially averaged to generate a one-dimensional radial flow profile. The turbulent length scale was determined by applying a spectral averaging as described by Wohlbrandt et al.[18] and Kissner et al.[9] The provided 1D turbulence statistics are shown in Figure 2.

B. Optimization of three-dimensional turbulence synthesis

One advantage of realizing three-dimensional turbulence is that all spatial correlations can be directly used. No equivalent 2D turbulence spectrum for the transverse fluctuating velocity component has to be determined

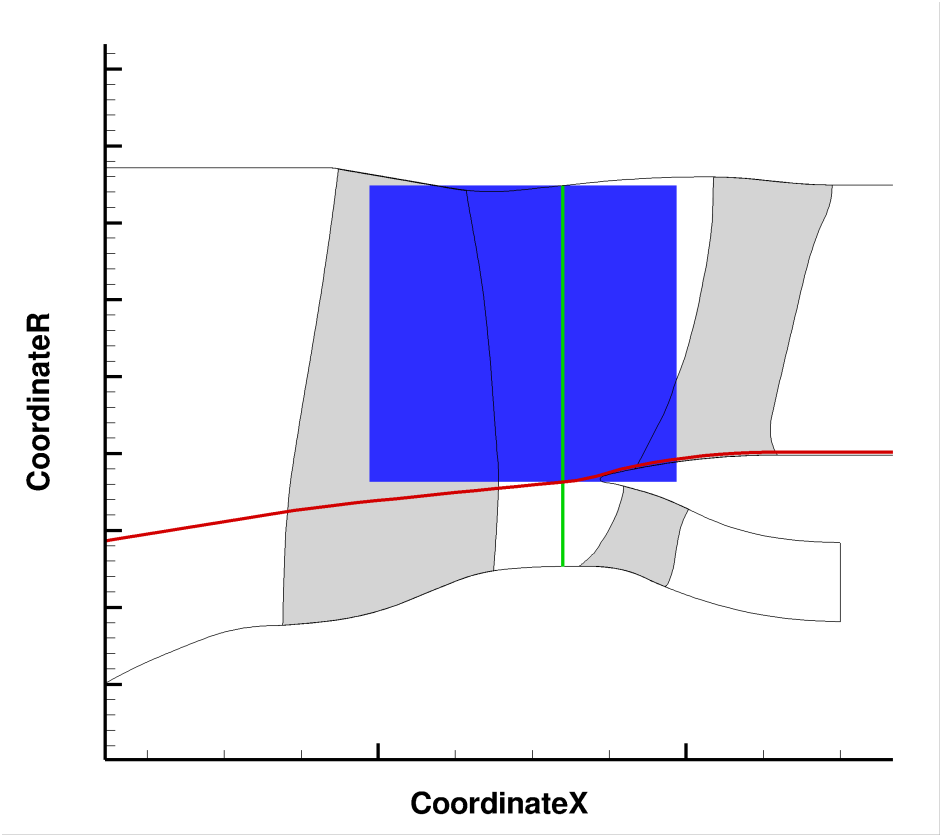

Figure 1. CFD domain containing rotor, stator, and ESS blades: The axial position of the extraction plane is marked in green and the streamline separating bypass and core flows, in red. The CAA domain to be used for applying the fRPM-fan method to this benchmark case is shown in blue.

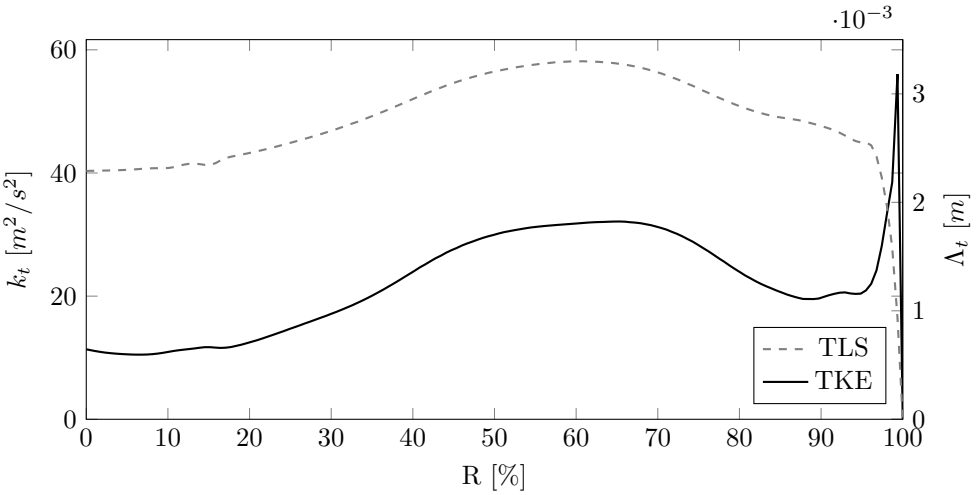

Figure 2. One-dimensional turbulence statistics: circumferentially averaged turbulent kinetic energy (TKE) and spectrally averaged turbulent length scale (TLS).

and thus no 2D to 3D turbulence correction is necessary when analyzing sound power spectra. However, one disadvantage is that the required computation cost tends to be significantly higher for a 3D simulation than for a 2D simulation. In past papers,[9,18] the chosen setup and mesh resolutions were chosen to be relatively conservative. For a 2D simulation, this approach is feasible as the computation cost is not yet critical. For a 3D simulation, a more optimized approach is required. As a first step, numerical and analytical parameter studies were performed to identify the key parameters that influence accuracy and cost for the turbulence synthesis and for the injection of the synthesized turbulence into to the CAA domain. The findings of these preliminary studies were then used to design a routine for optimizing these parameters for a given set of requirements. The analysis and studies presented in this section will be focused on examining the transverse velocity component as it is assumed to be the most relevant for the sound generation mechanism. This assumption is oftentimes made in analytical models and has also been numerically confirmed for certain airfoil types.[22]

Find citation for analytical models.

1. *Turbulence synthesis with fRPM method*

To pinpoint the most relevant factors for turbulence synthesis, a series of numerical and analytical parameter studies were conducted. These parameter studies were typically performed on a reduced version of the synthetic turbulence benchmark case.

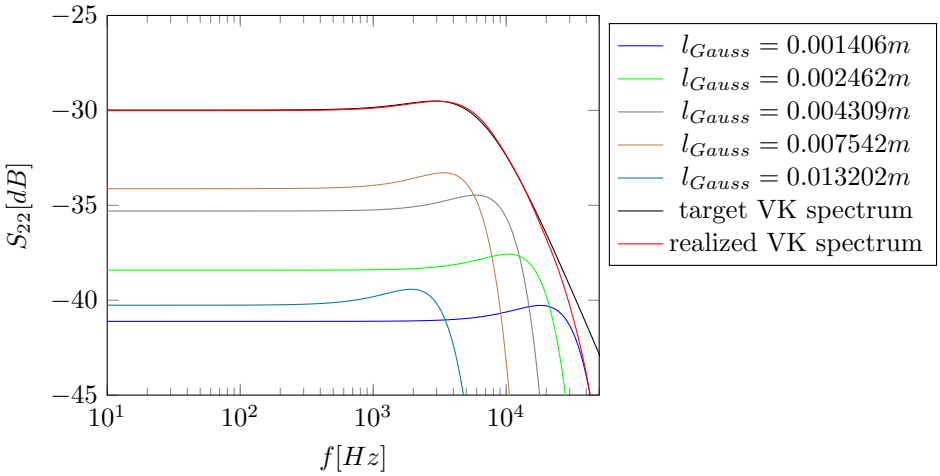

Figure 3. Superposition of Gaussian turbulence spectra for the realization of a target von Kármán turbulence spectrum

To synthesize a realistic turbulence spectrum such as a von Kármán turbulence spectrum, Gaussian filters are superposed to approximate a target spectrum. Essentially, a length scale l_m is prescribed for each Gaussian filter and weighted with a respective analytical weighting function $f(l)$. For further details regarding the technique and its realization and discretization for the Random Particle Mesh method, please refer to the work of Wohlbrandt et al.[12] An example of the superposition technique is shown in Figure 3. Five Gaussian turbulence spectra are used to realize the von Kármán spectrum using turbulence and flow characteristics at a radial position of 50%.

The goal of the turbulence synthesis is to accurately reconstruct turbulence at a reasonable cost. In the parameter studies, the following factors have been identified as having an influence on the overall computation cost of the turbulence synthesis:

- Number of cells of the fRPM patch: The fRPM patch is - as of now - not parallelized and therefore a key factor for the computation effort of the fRPM-fan method. The computation time is proportional to the number of fRPM cells.
- Cell size Δx_i: The largest possible time step is determined by the cell size via the CFL criterion. Smaller cells require smaller time steps and thus more total time steps have to be performed to reach a suitable sampling time.

- Number of Gaussian filters N_{Gauss}: Each additional Gaussian filter tends to increase the computation time by nearly a factor of 1.5 for three-dimensional applications.
- Particle density: Decreasing the particle density by a factor of 2 reduces the computation time by about 20%. The particles are convected along streamlines and are used to project variables onto the Cartesian fRPM grid. They are randomly distributed in the domain during the initialization process. When they exit the domain, they are "recycled" at the inflow of the fRPM domain. It is essential that the particles remain evenly distributed and that the overall particle density does not drop below one. An accumulation of particles can occur in boundary layers and near stagnation points, which can reduce the particle density in other regions of the domain to critically low levels. This has, however, not been observed for test cases using a realistic interstage flow. Therefore, a particle density slightly above one was targeted and the local particle density was closely monitored during simulations.

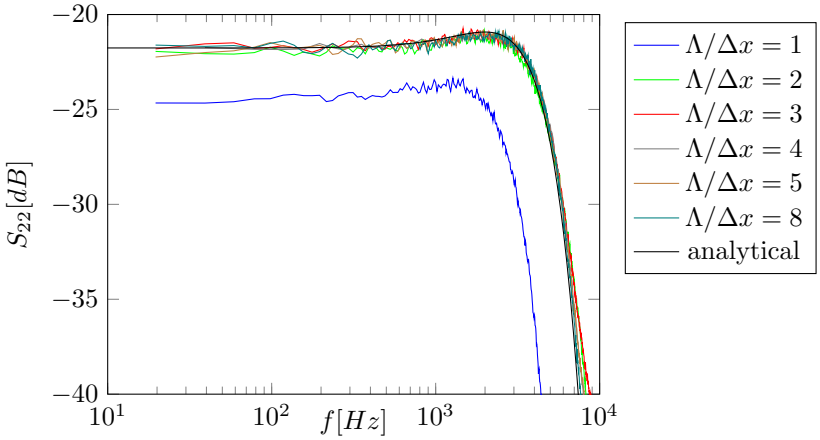

Figure 4. Variation of grid resolution for the realization of a target Gaussian turbulence spectrum

The most important factors that influence the accuracy of the turbulence synthesis are related to each other by the filter resolution:

$$FR = \frac{N_{Gauss}}{\log_{10}(l_{max}) - \log_{10}(l_{min})}, \tag{1}$$

where l_{max} denotes the **maximum Gaussian length scale** and l_{min} denotes the **minimum Gaussian length scale** used for the reconstruction of a target turbulence spectrum. The maximum Gaussian length scale should be greater than four times the maximum length scale Λ_{max}. Its maximum length is limited by the size of the fRPM domain in the transverse velocity direction, which is typically equal to the pitch between two stator blades. The minimum Gaussian length scale is related to the maximum **cell size** Δx_i in the fRPM domain. To ensure an adequate resolution, the minimum Gaussian length scale should be greater or equal to three times the limiting cell size. This relation is demonstrated in Figure 4. The cell size of a simple patch was varied, while the turbulent length scale ($\Lambda = 0.001m$), the turbulent kinetic energy ($k_t = 50m^2/s^2$), and the total velocity ($u_0 = 10m/s$) were kept constant. Gaussian spectra were realized. The results are identical for frequency spectra of all velocity components and seem to be independent of imposed turbulence statistics and velocities as suggested by additional tests. The **number of Gaussian filters** N_{Gauss} not only influences the computation cost but also the accuracy. Experience shows that the number of used Gaussian filters should be equal to or greater than four.

2. Injection of synthesized turbulence into CAA domain

The synthesized turbulence is solenoidally coupled into the CAA domain by the LEE-relaxation formulation.[16] A relaxation term is added to the impulse equations,

$$\frac{\partial u_i'}{\partial t} + \cdots = -\epsilon_{ijk}\frac{\partial}{\partial x_j}\left[\sigma\left(\Omega_k' - \Omega_k^{\text{ref}}\right)\right], \tag{2}$$

where σ is the forcing parameter, Ω'_k is the vorticity on the left hand side of this equation as

$$\Omega'_k = \epsilon_{ijk} \frac{\partial u'_k}{\partial x_j}, \tag{3}$$

and Ω_k^{ref} is the externally imposed fluctuating reference vorticity. The forcing parameter σ determines how strongly the synthesized turbulence is coupled into the CAA domain. This factor is most critical for an optimal turbulence injection.

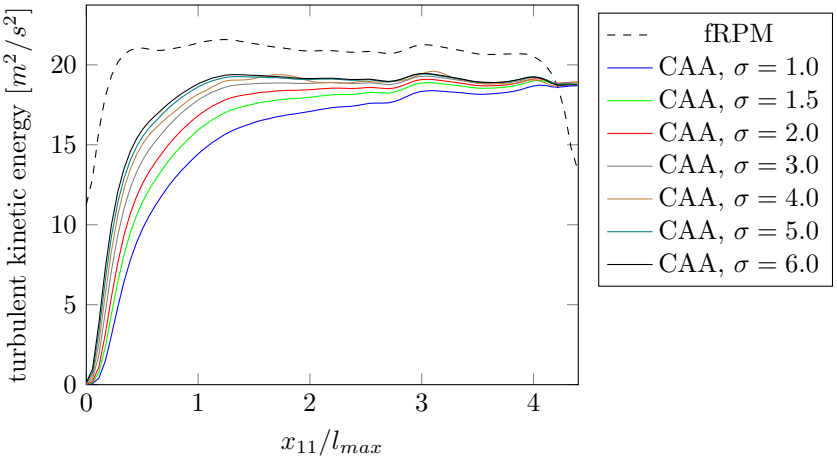

Figure 5. Influence of the relaxation parameter on LEE-relaxation coupling

In a first study, the forcing parameter was varied to investigate how quickly the synthesized turbulence is injected into the CAA domain. The instantaneous TKE was averaged over at least 1000 time steps in both fRPM and CAA domains at a radial position of 50%. In Figure 5, the averaged turbulent kinetic energy over the relative patch length in streamwise direction is shown. It can be seen that the variance increases in the CAA domain until it reaches a plateau at approximately 90% of the targeted value of turbulence level. The rate of increase grows as the forcing parameter is increased. A high forcing parameter is therefore desirable as the length of the patch could be decreased accordingly. This would result in a smaller patch, which would lower the computation costs. The drop in variance in the fRPM patch near its borders can be attributed to the fact that the larger length scales needed for the realization of the turbulence do not fit into that region and cannot be fully realized. This border region typically has a depth equal to the maximum length scale Λ_{max} of input turbulence. It should be noted that the variance of the turbulence synthesized in the fRPM domain is not completely reproduced in the CAA domain. This could be due to different grid resolutions in the fRPM and CAA domains.

Better way to explain this loss?

However, the forcing parameter cannot be chosen arbitrarily high since the forcing parameter is limited by stability considerations. Numerical tests of a reduced turbulence synthesis benchmark case were performed to identify a useful relation between stability and the forcing parameter. The results are shown in Figure 6. Stable simulations are indicated by green markers and unstable simulations, by red markers. A rule for the limiting case was identified:

$$\frac{\sigma}{\sigma_{Re}} < \frac{1.5}{\frac{\Delta t}{\Delta t_{fRPM}}}. \tag{4}$$

The forcing parameter σ_{Re} was derived by considering a Reynolds number $Re_{\Delta x}$ based on an averaged cell size $\overline{\Delta x}$:

$$Re_{\Delta x} = \frac{\overline{u_0}\,\overline{\Delta x}}{\sigma_{Re}} = 1. \tag{5}$$

The maximum time step Δt is related to the stability footprint of the fourth order low-dispersion low-dissipation Runge Kutta scheme[14] used by the CAA code:

$$\Delta t \leq \frac{2.83}{\pi} \frac{\Delta x}{u_0 + c}, \tag{6}$$

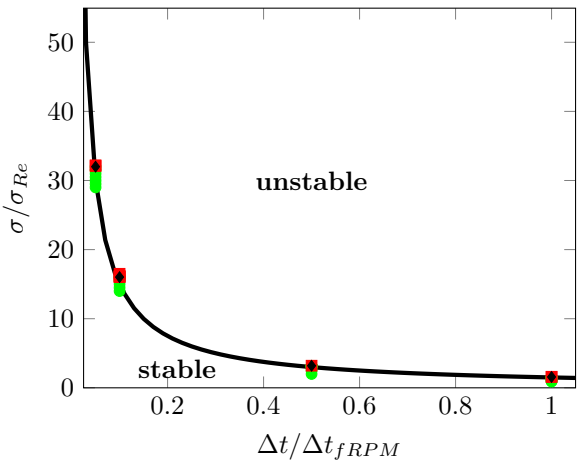

Figure 6. Numerically determined stability criterion of LEE-relaxation coupling

where c designates the speed of sound. The maximum time step Δt depends on the smallest cell size in the CAA domain. The time step Δt_{fRPM} is the critical time step if the smallest cell were located in the fRPM domain, i. e. the ratio $\frac{\Delta t}{\Delta t_{fRPM}}$ is equal to one if the grid resolutions in the fRPM and CAA domain are identical. For a generic test case, the $\frac{\Delta t}{\Delta t_{fRPM}}$ is, in fact, close to one. For a realistic fan configuration, the smallest cell size in the CAA domain is typically located at the leading edges of the OGV's and is significantly smaller than the cell size used in the turbulence injection region. The ratio $\frac{\Delta t}{\Delta t_{fRPM}}$ is typically close to 0.1 for realistic cases. Note that the maximum time step Δt_{max} of the CAA code is always more critical than the maximum time step permitted by the fRPM method. The fRPM time step is limited by a convective stability criterion, while the CAA time step is limited by a criterion that considers convection and acoustics.

Equation 4 implies that higher forcing parameters can be chosen if the time step is reduced. However, this is usually not practical as it increases the overall computation time. Instead, the maximum permissible time step should be used and the maximum forcing parameter should be chosen as large as the ratio $\frac{\Delta t}{\Delta t_{fRPM}} \approx \frac{\Delta x_{min,CAA}}{\Delta x_{fRPM}}$ allows.

The authors are working on finding an analytically derived expression that confirms the stability criterion found by Equation 4.

Prove stability criterion analytically.

3. Description of optimization routine

Visualize work flow for future paper?

Since numerous factors - including respective limitations - play a role in terms of accuracy and computation time, an optimization routine was programmed rather than to do a manual optimization. The optimization routine is designed to optimize the transverse velocity frequency spectrum and will be discussed for the synthetic turbulence benchmark case.

The routine works as follows:

1. Definition of accuracy targets: The user provides a maximum target frequency and an allowed offset between the target and superposed spectrum. The offset is negative if the superposed spectrum lies below the target spectrum and vice versa. The maximum positive and the minimum negative offsets essentially defines a corridor around the target spectra. For the benchmark test, the maximum target frequency was set to 10000 Hz, the maximum positive offset to 1.0 dB, and the minimum negative offset to -0.1 dB. The maximum target frequency was chosen so that the peak frequency of the turbulence spectrum is well within the frequency range. The offsets are to be fulfilled at all frequencies and were chosen to account for the fact that a bit of energy tends to be lost in the turbulence injection. A positive offset is therefore preferred.

2. Definition of case-specific constant: The number of stator blades, a target patch length (considering coupling in and stability considerations), and the considered radial positions need to be specified. The target patch length was set to $2.5 \cdot l_{max}$, since the grid resolutions in the CAA and fRPM domains will be nearly equal and thus a maximum forcing of $\sigma < 1.5$ is allowed. The specified radial position were at 10%, 20%, 30%, 40%, 50%, 60%, 70%, 80%, and 90% and ensure that the accuracy targets are met over entire span. In addition, search ranges for N_{Gauss}, l_{max}, l_{min}, and Δx_i can be adjusted. Note that parameter limitations are enforced regardless of the defined ranges.

3. Search for members: For each cell size and radial position, l_{min}, l_{max}, and N_{Gauss} are optimized consecutively. Members that fulfill the accuracy requirements are saved and a computation cost (considering all relevant factors mentioned in Section 1) is estimated. After each optimization step, the cell size is adjusted. If no more members can be found, the search for members is terminated.

4. Finding optimal settings: Lastly, the routine searches for the eligible member that requires the least computation effort.

Possibly show optimization routine in dependence of filter resolution: Could explain dependence of optimal filter resolution on chosen accuracy offsets. Could visualize relation between cell size and maximum frequency.

Table 1. fRPM/CAA settings determined with optimization routine and with previous best practice approach

	$f_{max}[Hz]$	$\Delta x_i[m]$	l_{min}	l_{max}	N_{Gauss}	FR	t_{rel}
with optimization	10000	0.001175	$3 \cdot \Delta x_i$	$10.75 \cdot \Lambda_{max}$	4	3.99	1.0
with optimization	20000	0.000825	$3 \cdot \Delta x_i$	$9.5 \cdot \Lambda_{max}$	4	3.63	3.6
no optimization	10000	0.00055	$2 \cdot \Delta x_i$	$4 \cdot \Lambda_{max}$	7	6.49	13.9
no optimization	20000	0.00038	$2 \cdot \Delta x_i$	$4 \cdot \Lambda_{max}$	7	5.65	59.8

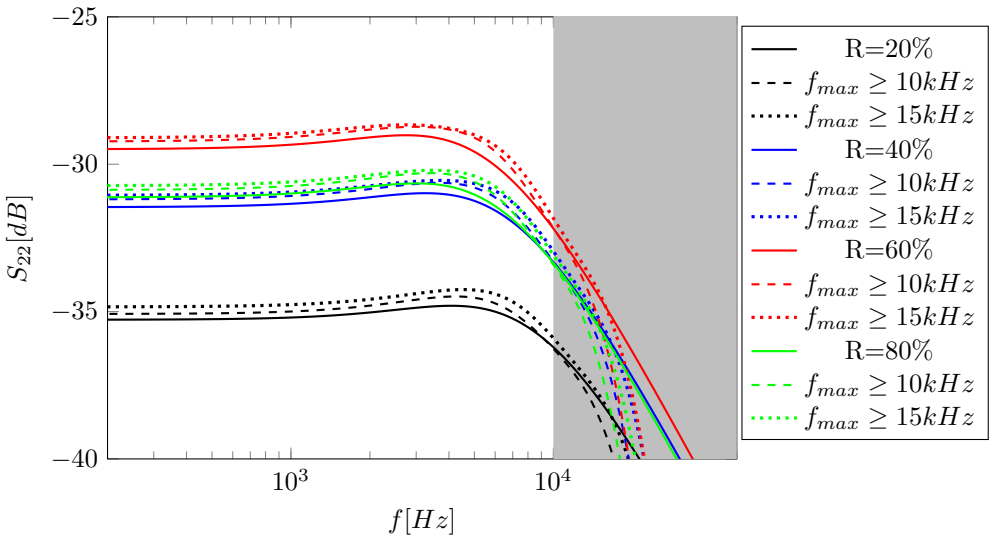

Figure 7. Realized transverse velocity frequency spectra at different radial positions for $f_{max} \geq 10000Hz$. The target spectra are shown as solid lines, while the realized spectra are dashed.

The optimization routine was applied with $f_{max} \geq 10000Hz$ and $f_{max} \geq 20000Hz$ and compared to settings using best practice guidelines that were applied in the past.[9,18] Table 1 shows that the optimization routine produces settings that should accelerate the simulation by more than a factor t_{rel} of 10 for both target frequencies. Since resolving up to a target frequency of 10000 Hz is cheaper by about a factor of 3.6 compared to resolving up to a target frequency of 20000 Hz and the peak frequency is approximately 5000 Hz, settings for $f_{max} \geq 10000Hz$ will be applied for the synthetic turbulence benchmark test. The realized

spectra are shown in Figure 7. The CAA domain will span three rotor passages in order to fit the fRPM patch.

C. fRPM/CAA setup for synthetic turbulence benchmark case

The previously determined optimal settings will be used to set up the fRPM and CAA domains for the synthetic turbulence benchmark case. The fRPM patch is rotated into the direction of the flow at each radial position. Only in the boundary layer, the rotation does not match the flow direction in order to avoid a largely distorted fRPM patch. Multiple sensors for analyzing the simulation are placed in both CAA and fRPM domains. The setup is shown in Figure 8.

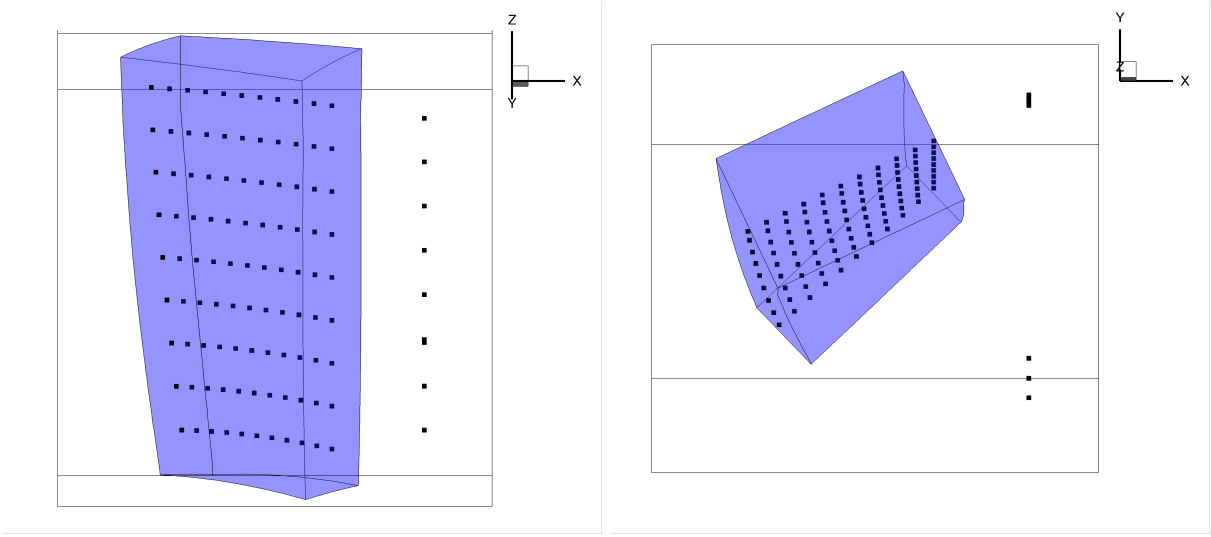

Figure 8. fRPM/CAA setup as viewed from the side (on the left) and from the top (on the right). The rotated fRPM patch (in blue) is shown inside the CAA domain. The sensor positions are marked by black dots.

D. Comparison of synthesized and analytical turbulence

In this section, the synthesized turbulence is compared to the analytical turbulence. The comparison is intended for the validation of the three-dimensional turbulence synthesis.

When analyzing the realized turbulence in the transverse velocity component, the targets are fulfilled. The realized S_{22} turbulence spectra in the fRPM and CAA domain match the analytical spectra as can be seen in Figure 9. The mean offsets between analytical and realized spectra are constant across the radius (see Figure 10). The offset for realized fRPM spectra is approximately 0.2 dB, while the offset for realized CAA spectra is approximately 0.5 dB. The loss between fRPM and CAA is acceptable as this is mostly due to the injection.

The results for the fluctuating streamwise and radial components are, however, more worrisome. The realized streamwise velocity frequency spectra drop off earlier than the targeted maximum frequency of 10000 Hz. This is expected as the optimization routine is applied to the transverse velocity component. Applying this routine to the streamwise velocity component results in smaller cell sizes. Since it is assumed that the fluctuating transverse velocity component is most critical for the noise generation mechanism, this faster drop-off at frequencies below the target frequency is acceptable. The high offset at lower frequencies, particular at higher radial positions, for both radial and streamwise velocity component was not expected. The reasons are still unclear and need to be identified before applying the method to an actual fan stage. However, the authors have tested that these problems do not occur for an untwisted fRPM patch with constant mean flow and turbulence statistics. The authors intend to start from the observation and incrementally increase the complexity of the test case to pinpoint the cause for the differences in realized and analytical spectra in the streamwise and radial directions.

For benchmark and possibly insert into paper: rms values of the velocity components, correlation length scales, velocity cross-spectra

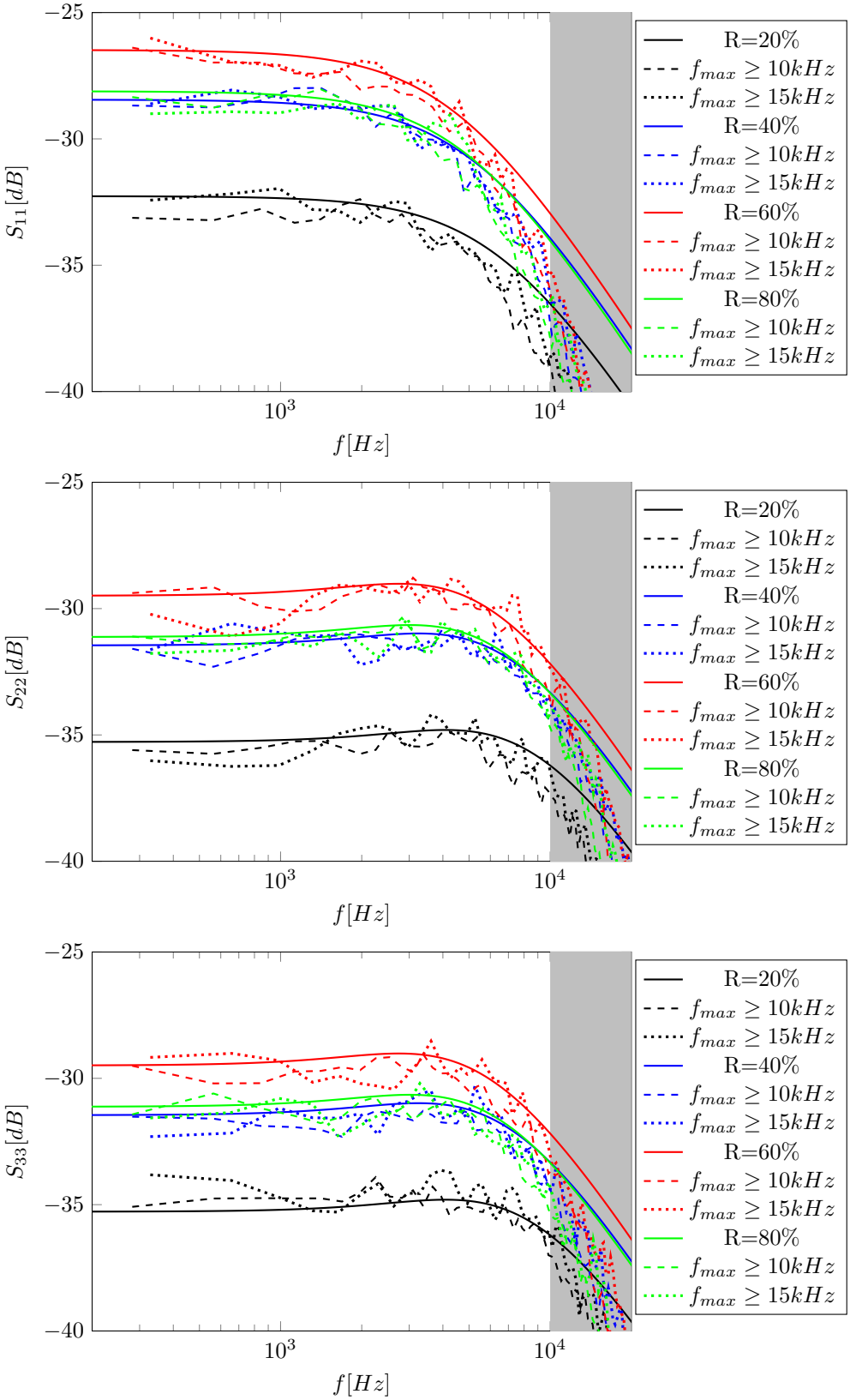

Figure 9. Comparison of numerically computed and analytical turbulence spectra. Synthesized fRPM spectra are shown by solid lines and CAA spectra, by dashed lines.

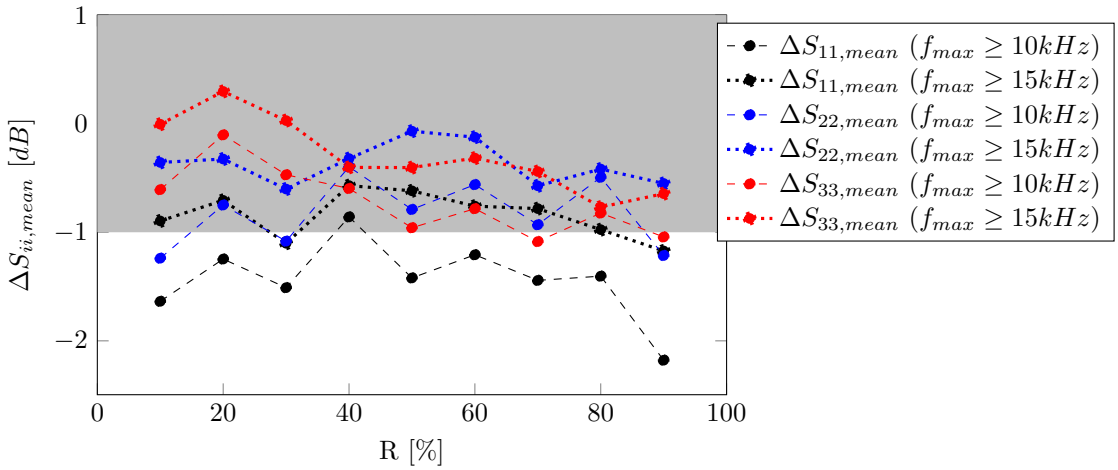

Figure 10. Mean offset between target and realized turbulence spectra shown as a function of the relative radius

For benchmark and possibly insert into paper: comparison at two axial positions in CAA domain

Find reason for offsets.

IV. Fan broadband noise prediction with 3D approach

In this section, the three-dimensional fRPM-fan method was applied for the prediction of the ACAT1 fan noise. In first step, the CFD simulation that was used as an input for method will be discussed. The fRPM/CAA setup will then be shown. The results of the method will be discussed and compared to the results of an equivalent two-dimensional simulation. Lastly, a comparison with experimental data will be performed. The ACAT1 fan was tested at the ANECOM UFFA facility during the TurboNoiseBB project. Details regarding the experimental setup are described by Guérin et al.[23] and Meyer et al.[24]

A. CFD input

For this work, the turbulence statistics and mean flow were extracted from a URANS simulation. Note that the used fRPM-fan approach does not require an unsteady solution. A steady solution would be suitable as well. The authors chose to use the URANS simulation for two reasons: 1.) The fRPM-fan method in combination with the URANS simulation allows for the prediction of the entire rotor-stator-interaction noise: tones (URANS) and broadband noise (fRPM-fan). 2.) The same simulation can be used for future investigation focusing on cyclostationary and anisotropic turbulence in the wakes. This also means that if tones are computed numerically, it automatically produces all inputs necessary for the simulation of the broadband noise mechanism.

The URANS simulation of the ACAT1 was performed at approach conditions using the DLR in-house CFD solver TRACE.[19] The SSG/LRR-ω full Reynolds stress turbulence model[25] was applied. One advantage of this model is that it computes realistic, anisotropic turbulence, which will be interesting for future investigations. The other advantage is that it is particularly suited for considering ingestion turbulence. Many two-equation turbulence models have an unrealistically high dissipation rate and cannot maintain ingested turbulence when passing through the rotor blades. This is particularly critical if the ingested turbulence does not have a negligibly small turbulence intensity or turbulent length scale. In this case, turbulence spectra measured by hot wire probes were fitted with von Kármán spectra to determine turbulence statistics. Outside of the boundary layer, the turbulence intensity was about 0.3% and the turbulent length scale was about 0.04 m. This turbulence along with flow conditions extracted from pressure rakes in the inlet were prescribed to match test conditions and ensure the correct thickness of the boundary layer.

The computation domain was reduced to the bypass as the investigation will focus on the interaction noise between rotor blades and OGV's. The bypass and core flows were separated by computing a streamline at the stator hub for a RANS simulation performed at the same operating conditions. The reduced domain

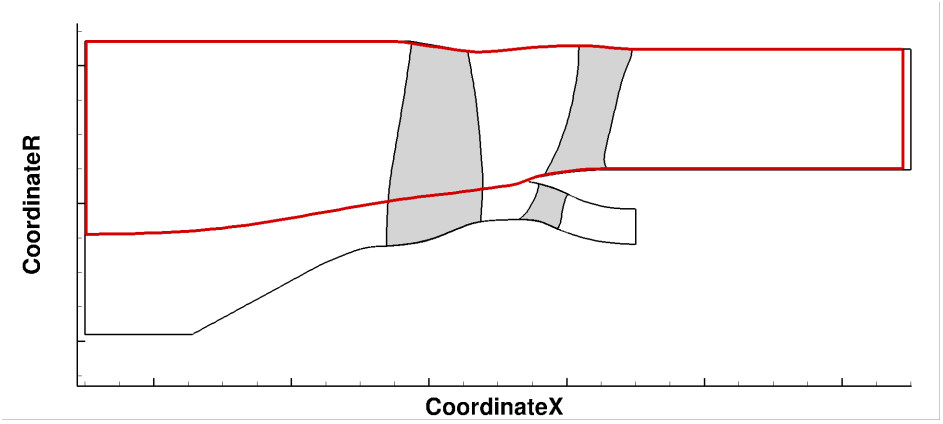

Figure 11. URANS Domain

is shown in red in Figure 11. Since phase-lag conditions in combination with the chosen turbulence model are not yet available, periodic boundary conditions are applied. The computation domain thus contains 4 rotor blades and 11 OGV's. During the mesh generation process, great care was taken to fully resolve wakes and boundary layers. The resulting mesh contains about 30 million cells and should suffice for the prediction of fan tones.

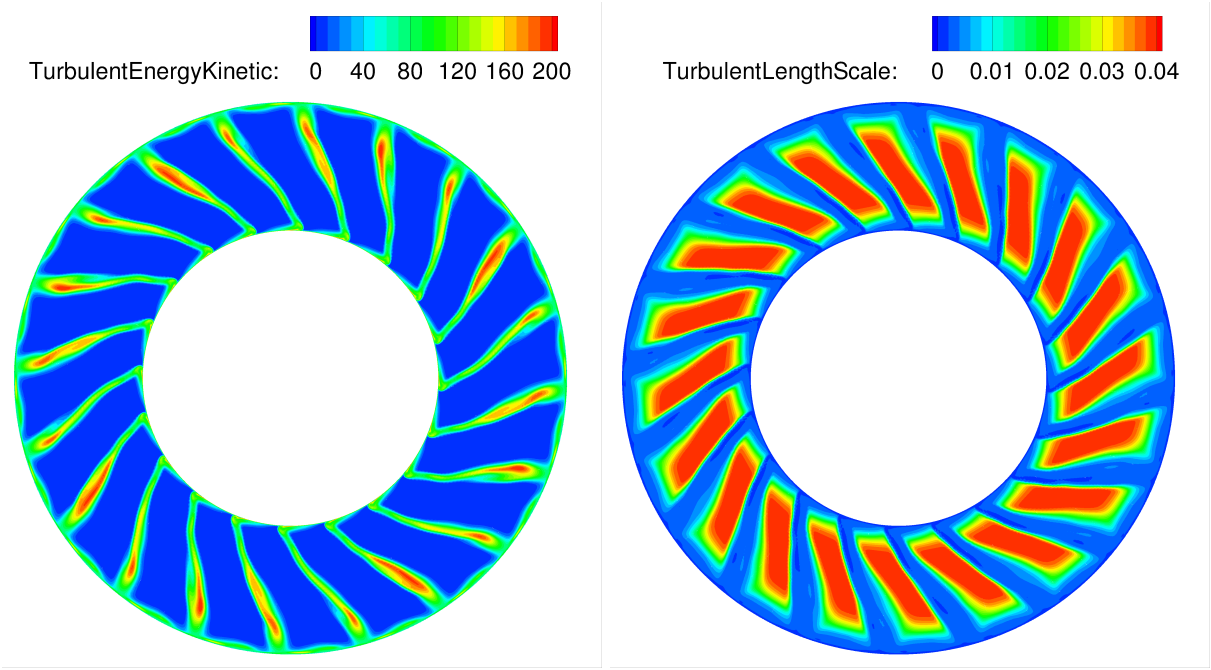

Figure 12. Instaneous turbulent kinetic energy (on the right) and turbulent length scale (on the left) at the axial position of the interstage hot wire probes

The URANS simulation is currently running but close to convergence. An impression of the instantaneous turbulent kinetic energy and turbulent length scale is shown in Figure 12. Hot wire measurement data in the interstage region is available and will be used to evaluate the simulation. In addition, the rotor-stator-interaction tones will be shown.

Comparison to HW data.

Insert table containing tones.

B. Setup of fRPM-fan simulation

In this section, the setup of the three-dimensional fRPM-fan simulation will be presented. A particular focus will be the discussion of turbulent and acoustic mesh resolution requirements.

- computation cost

1. Turbulent mesh resolution

2. Acoustic mesh resolution

C. Discussion of results

In this section, the results of the three-dimensional simulation will be analyzed.

D. Comparison to an equivalent 2D fRPM-fan simulation

In this section, a new method for designing an equivalent 2D fRPM-fan simulation will be introduced. The sound power level spectra of the 2D simulation will then be compared to results of the 3D simulation.

... more complete description of problem using three simulations at different radial positions indicate that total results are close to 50% cut[9]

confirms results found for NASA SDT fan[18]

- analyze turbulence in interstage area, contribution of background, bl, wake, total
- which streamline location
- determination of radial flow:

$$\overline{\rho_0^2 u_0^2} = \frac{1}{n}\sum_{i=1}^{n} \rho_0(r_i)^2 u_0(r_i)^2 \tag{7}$$

-determination of equivalent radial turbulence:

$$\overline{S_{22}} = \frac{\frac{1}{n}\sum_{i=1}^{n} \rho_0(r_i)^2 u_0(r_i)^2 S_{22}(r_i, f)}{\overline{\rho_0^2 u_0^2}} \tag{8}$$

- fit $\overline{S_{22}}$ with VK spectrum and with radial flow $\overline{u_0}$ to determine tke and tls
- set up 2D simulation on streamline position matching radial flow average and using fitted turbulence statistics

E. Comparison to experimental data

In this section, simulation results will be compared to experimental data. The The experimental sound power level spectrum were computed using line array of condensor microphones located in the bypass duct downstream of the fan stage. To separate acoustic from hydrodynamic pressure fluctuations, the microphone signals were filtered using an axial wavenumber decomposition technique.[26] A cyclostationary analysis was applied to remove the rotor-locked components in order to isolate the broadband noise.[27] The sound power was then estimated under the assumption of equal energy distribution between the propagating modes of the same frequency band. The sound power level spectrum of the ACAT1 fan at approach conditions has been presented by Guérin et al.[23]

V. Conclusion

TBC...

in future: take into account cyclostationarity for 3D simulation; investigate anisotropy in wakes (makes most sense for 3D)

Funding Sources

The presented work was conducted in the frame of the project TurboNoiseBB, which has received funding from the European Union's Horizon 2020 research and innovation program under grant agreement No. 690714.

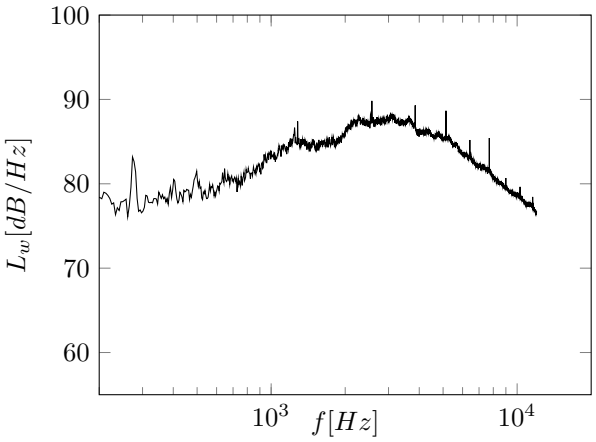

Figure 13. Sound power level spectrum determined by using measurement in bypass duct

Acknowledgements

The authors thank Roland Ewert, Jürgen Dierke, and Nils Reiche (DLR) for their continued support and advice.

References

[1]Ewert, R., "Broadband slat noise prediction based on CAA and stochastic sound sources from a fast random particle-mesh (RPM) method," *Computers & Fluids*, Vol. 37, No. 4, 2008, pp. 369–387.

[2]Dieste, M., *Random-vortex-particle methods applied to broadband fan interaction noise*, Ph.D. thesis, University of Southampton, 2011.

[3]Kraichnan, R. H., "Diffusion by a random velocity field," *Physics of Fluids (1958-1988)*, Vol. 13, No. 1, 1970, pp. 22–31.

[4]Bechara, W., Bailly, C., Lafon, P., and Candel, S. M., "Stochastic approach to noise modeling for free turbulent flows," *AIAA Journal*, Vol. 32, No. 3, 1994, pp. 455–463.

[5]Billson, M., Eriksson, L.-E., and Davidson, L., "Jet noise prediction using stochastic turbulence modeling," *9th AIAA/CEAS Aeroacoustics Conference*, Hilton Head, South Carolina, 2003.

[6]Jarrin, N., Benhamadouche, S., Laurence, D., and Prosser, R., "A synthetic-eddy-method for generating inflow conditions for large-eddy simulations," *International Journal of Heat and Fluid Flow*, Vol. 27, No. 4, Aug. 2006, pp. 585–593.

[7]Sescu, A. and Hixon, R., "Toward low-noise synthetic turbulent inflow conditions for aeroacoustic calculations," *International Journal for Numerical Methods in Fluids*, Vol. 73, No. 12, 2013, pp. 1001–1010.

[8]Kim, J. W. and Haeri, S., "An advanced synthetic eddy method for the computation of aerofoil-turbulence interaction noise," *Journal of Computational Physics*, Vol. 287, 2015, pp. 1–17.

[9]Kissner, C. A., Wohlbrandt, A. M., and Guérin, S., "Enhanced Fan Broadband Noise Prediction Based on a 2D Synthetic Turbulence Method," *24th AIAA/CEAS Aeroacoustics Conference*, American Institute of Aeronautics and Astronautics, 2018.

[10]Ewert, R., Dierke, J., Siebert, J., Neifeld, A., Appel, C., Siefert, M., and Kornow, O., "CAA broadband noise prediction for aeroacoustic design," *Journal of Sound and Vibration*, Vol. 330, No. 17, 2011, pp. 4139–4160.

[11]Siefert, M. and Ewert, R., "Sweeping Sound Generation in Jets Realized with a Random Particle-Mesh Method," *15th AIAA/CEAS Aeroacoustics Conference*, 2009.

[12]Wohlbrandt, A., Hu, N., Guérin, S., and Ewert, R., "Generalised turbulence spectra for broadband noise predictions with the Random Particle Mesh method," *Computers and Fluids*, Vol. 132, 2016, pp. 46–50.

[13]Delfs, J. W., Bauer, M., Ewert, R., Grogger, H., Lummer, M., and Lauke, T., "Numerical Simulation of Aerodynamic Noise with DLR's aeroacoustic code PIANO," Tech. rep., German Aerospace Center (DLR), Braunschweig, Jan. 2008.

[14]Hu, F. Q., Hussaini, M. Y., and Manthey, J. L., "Low-dissipation and low-dispersion Runge - Kutta schemes for computational acoustics," *Journal of Computational Physics*, Vol. 124, No. 1, 1996, pp. 177–191.

[15]Tam, C. K. and Webb, J. C., "Dispersion-relation-preserving finite difference schemes for computational acoustics," *Journal of Computational Physics*, Vol. 107, No. 2, 1993, pp. 262–281.

[16]Ewert, R., Dierke, J., Neifeld, A., and Moghadam, S. A., "Linear-and Non-Linear Perturbation Equations with Relaxation Source Terms for Forced Eddy Simulation of Aeroacoustic Sound Generation," *AIAA Paper*, Vol. 3053, 2014.

[17]Wohlbrandt, A., Guérin, S., and Ewert, R., "Extension of the Random Particle Mesh method to periodic turbulent flows for fan broadband noise prediction," *AIAA paper 2015-2383, 21st AIAA/CEAS Aeroacoustics Conference*, 2015.

[18]Wohlbrandt, A., Kissner, C., and Guérin, S., "Impact of cyclostationarity on fan broadband noise prediction," *Journal of Sound and Vibration*, Vol. 420, April 2018, pp. 142–164.

[19]Becker, K., Heitkamp, K., and Kügeler, E., "Recent Progress in a Hybrid Grid CFD Solver for Turbomachinery Flows," *Proc. V European Conference on Computational Fluid Dynamics ECCOMAS CFD 2010*, Lisbon, Portugal, 2010.

[20]Menter, F. R., "Two-equation eddy-viscosity turbulence models for engineering applications," *AIAA Journal*, Vol. 32, No. 8, 1994, pp. 1598–1605.

[21]Tam, C. K. and Auriault, L., "The wave modes in ducted swirling flows," *Journal of Fluid Mechanics*, Vol. 371, 1998, pp. 1–20.

[22]Gill, J., Zhang, X., Joseph, P., and Nodé-Langlois, T., "Reduced dimension modeling of leading edge turbulent interaction noise," *20th AIAA/CEAS Aeroacoustics Conference*, 2014.

[23]Guérin, S., Kissner, C., Kajasa, B., Jaron, R., Behn, M., Hakansson, S., Pardowitz, B., Tapken, U., Meyer, R., and Enghardt, L., "Trends in fan broadband noise of the ACAT1 fan," 25th AIAA/CEAS Aeroacoustics Conference, Delft, Netherlands, 2019.

[24]Meyer, R., Hakansson, S., Hage, W., and Enghardt, L., "Instantaneous flow field measurements in the interstage section between a fan and the outlet guiding vanes at different axial positions," 13th European Conference on Turbomachinery Fluid Dynamics and Thermodynamics, Lausanne, Switzerland, 2019.

[25]Cécora, R.-D., Radespiel, R., Eisfeld, B., and Probst, A., "Differential Reynolds-stress modeling for aeronautics," *AIAA Journal*, 2015.

[26]Tapken, U., Pardowitz, B., and Behn, M., "Radial mode analyis of fan broadband noise," 23rd AIAA/CEAS Aeroacoustics Conference, Denver, Colorado, USA, 2017.

[27]Behn, M., Pardowitz, B., and Tapken, U., "Separation of tonal and broadband noise components by cyclostationary analysis of the modal sound field in a low-speed fan test rig," Fan2018, Darmstadt, Germany, 2018.